Investigation of Spot Weld Behavior Using Detailed Modeling Technique

Falko Seeger, Guillaume Michel, Matthieu Blanquet
Daimler AG, GR/VCS, HPC X603, 71059 Sindelfingen, Germany
falko.seeger@daimler.com

Summary:

The development of suitable and robust simplified spot weld models for full vehicle crash simulation meets one of the major demands of the development process regarding efficient and appropriate full car crash models. Normally a high number of experiments are required to derive and validate accordant material and failure parameters for each material and gage combinations. Concerning systematical investigations, the effort for manufacturing and testing can increase immoderately.

In this paper, we describe a method to reduce the effort of characterizing the joint failure by using a highly detailed simulation model. Different loading conditions and geometrical aspects can be analyzed by using this model in combination with the Gurson's material model as an appropriate visco-plastic material model which includes already a damage formulation. Especially the experimental investigation of strain rate effects at higher velocities of joints is quite sophisticated due to dynamic effects of the test arrangement – the magnitudes are often overlaid by oscillations. Using the simulation to evaluate the behavior of a spot weld allows to study and predict the strain rate effect for higher velocities. As a second point, we use the detailed model for a systematic analysis to determine the effect of the sheet thickness with respect to the failure parameters. The influence of imperfections which occurs due to the production process can be eliminated, so that a self-contained approach can be obtained.

Keywords:

Spot weld modeling, detailed model, crash worthiness, finite element method

1 Introduction

Today, the entire body in white contains a few thousand spot welds joining different material and gage combinations. To cover the behavior of all possible combinations in the car crash simulation, a great number of experiments are necessary. Especially the systematical analysis of the main parameters, such as sheet thickness and load speed, are required for each material combination an accordant distribution of supporting points. To reduce the cost and time to perform experiments, a detailed model of a spot weld was developed. If the model is fine enough the real effects can be simulated.

The utilization of a detailed spot weld model provides a number of advantages, however two main points are emphasized in this paper. On one hand the effort for such systematical analysis can be reduced; on the other hand the quality could be improved, since the spot weld and the heat affected zone can be modeled perfectly. Disturbances, which occur normally during the welding process, would be avoided and variations are minimized. Mainly, dynamic experiments with higher load speed are affected by dynamic effects of the testing machine and the clamping devices, which cause oscillations in the measured quantities.

2 Experimental Basis

For deriving suitable and robust simplified models a series of experiments on coupon level need to be performed. In recent years the tensile-shear specimen, called KS2-specimen, the coach peel and a simple lap shear were developed for testing different kinds of joining technologies, see Fig. 1. The KS2 is subjected to different load angles, so that tensile and shear loading as well as a combination of both can be submitted and investigated.

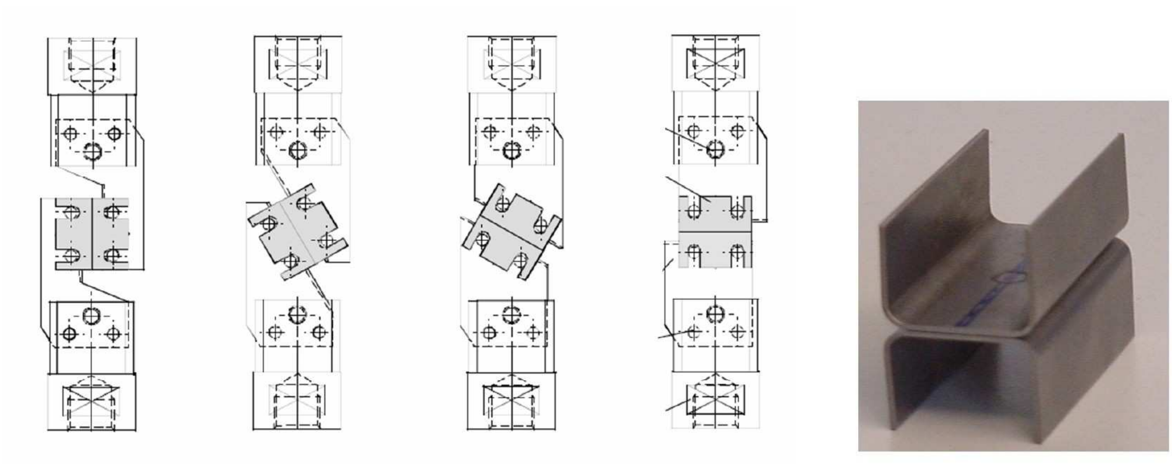

(a) load angles of 0°, 30°, 60° and 90° (b) KS2-specimen

Figure 1: KSII-specimen

The experimental basis on coupon level is completed by the coach peel and the simple lap shear. In general, all specimens can be subjected to different load speeds from quasi-static to 2 m/s. For later investigations the resultant force as well as the displacement are measured.

3 Modeling of the Spot Weld

3.1 Geometry

The accurate modeling of the real spot weld geometry provides the basis for a good correlation of experimental data and numerical results. Only if the degree of detailing is sufficiently high enough, the behavior of the spot weld failure can be simulated as best as possible. For this purpose, a cut and a Vickers hardness test will be performed for a untested spot weld exemplary for a complete test series of a given material/gage combination. Fig. 2 shows a cut for the HT600XD in combination with the corresponding Vickers hardness test. At a first glance, the three different sub-zones: basic material (BM), heat affected zone (HAZ) and spot weld (SW) can be identified by the characteristic of the hardness.

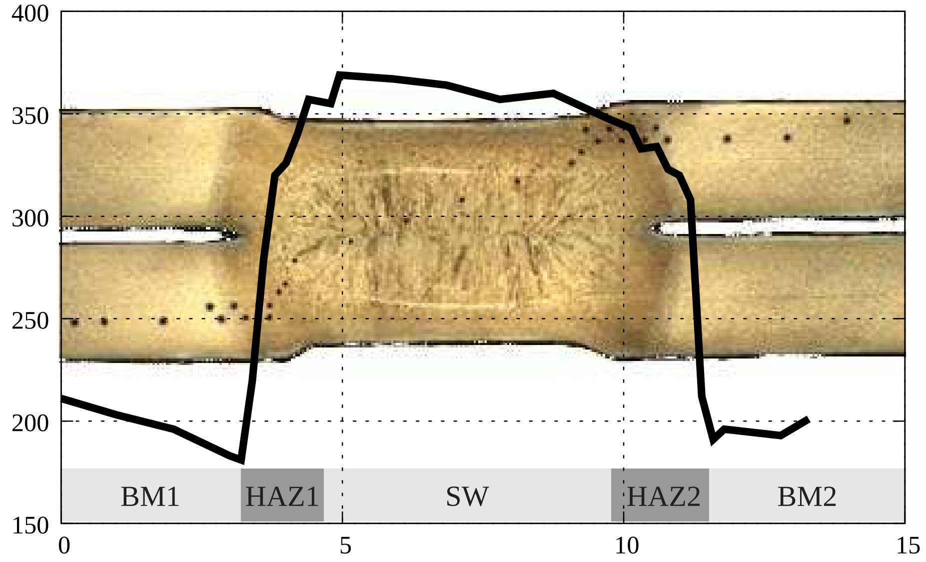

Figure 2: Cut of a spot weld (HT600XD) with corresponding Vickers hardness test

With the dimension determined for each sub-zone of the spot weld, the geometry and the finite element mesh can be build for the given specimen. Hence the number of elements is limited by a meaningful simulation time, the size of a single element should not be less than 0.25 mm per edge. With this dimension of a hexahedron element, a sheet is modeled by a range from 4 to 8 elements for a thickness of 1 mm to 2 mm respectively, see Fig. 3.

In the second step, the material parameters of the heat affected zone and the spot weld has to be determined. Therefore the Vickers hardness test is used for scaling the stress-strain-curve of the heat affected zone as well as the spot weld on basis of the basic material.

3.2 Material model

The second comparable important part in modeling is the choice of a suitable material model and the validation of the relevant material parameters. Among all available material models implemented currently in LS-Dyna, the Gurson model seems to be the best capable one. This material model adapts an elasto-viscoplastic formulation with an included damage model which is based on the existence and the evolution of pores inside the material [4, 7]. This model was implemented in LS-Dyna in the late 1990s and enhanced by strain rate dependent behavior, [2, 3].

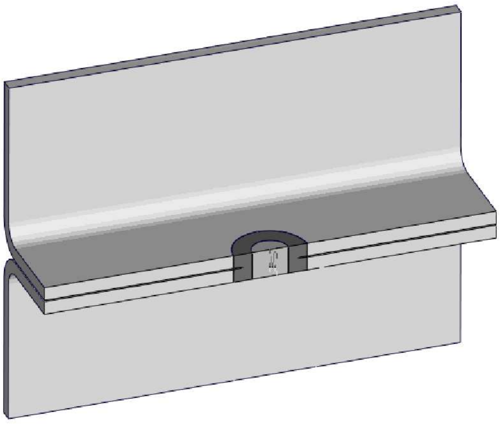

(a) Cut of a detailed model of a KS2-specimen

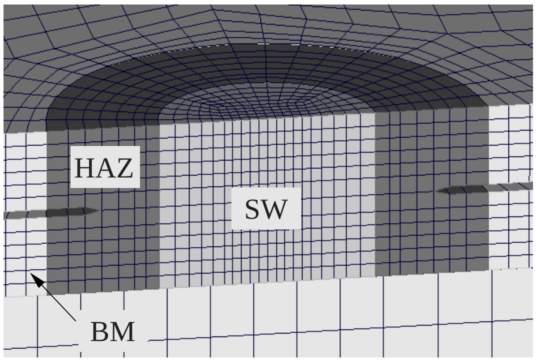

(b) Model of the 3 sub-zones of the spot weld

Figure 3: Detailed Model of Spot Weld

To derive the material parameter or the yield curve for the heat affected zone and the spot weld, the DIN 50 150 was used, which includes the relation between hardness and the tensile strength, see Fig. 4a. With the corresponding tensile strength for the basic material, heat affected zone and spot weld the scaling factors follow by

$$\beta_{HAZ} = \frac{R_m^{(HAZ)}}{R_m^{(BM)}} \quad \text{and} \quad \beta_{SW} = \frac{R_m^{(SW)}}{R_m^{(BM)}}.. \tag{1}$$

With Eq. (1) the yield curves of all zones can be written as

$$\sigma^{(HAZ)}(\varepsilon,\dot{\varepsilon}) = \beta_{HAZ}\,\sigma^{(BM)}(\varepsilon,\dot{\varepsilon}) \quad \text{and} \quad \sigma^{(SW)}(\varepsilon,\dot{\varepsilon}) = \beta_{SW}\,\sigma^{(BM)}(\varepsilon,\dot{\varepsilon}) \tag{2}$$

Alternatively, the material parameters could be determined from small tensile test excised from real spot welds or made by Gleeble's method [10]. But these methods are connected partly with inaccuracies and imply high effort in manufacturing and testing. Furthermore, the modification of the rupture strain of

	Tensile strength Rm in N/mm^2	Vickers hardness HV ($F \sim 98$ N)
	545	170
BM	575	180
	610	190
	⋮	⋮
	1095	340
SW	1155	360
HAZ	1220	380
	1290	400

(a) Content of DIN 50 150

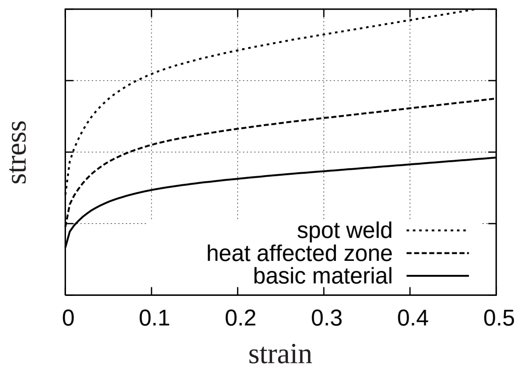

(b) Yielding curves of all sub-zones

Figure 4: Material parameter for the detailed model

the heat affected zone and the spot weld should be taken into account too. In general, the increase of the tensile strength causes a decrease of the rupture strain. Since there are no reliable and accurate data available this effect was neglected.

3.3 Simplified model

Because of the limitation of the numerical model of a body in white regarding the computational effort, the spot weld can only simulated efficiently with simplified models [8, 9]. Currently a cluster with 4 or 8 hexahedron elements has to be established to model the spot weld behavior. As a suitable material model for the hexahedron cluster a bi-linear, elasto-plastic material was chosen and implemented in MAT_SPOTWELD_DA.

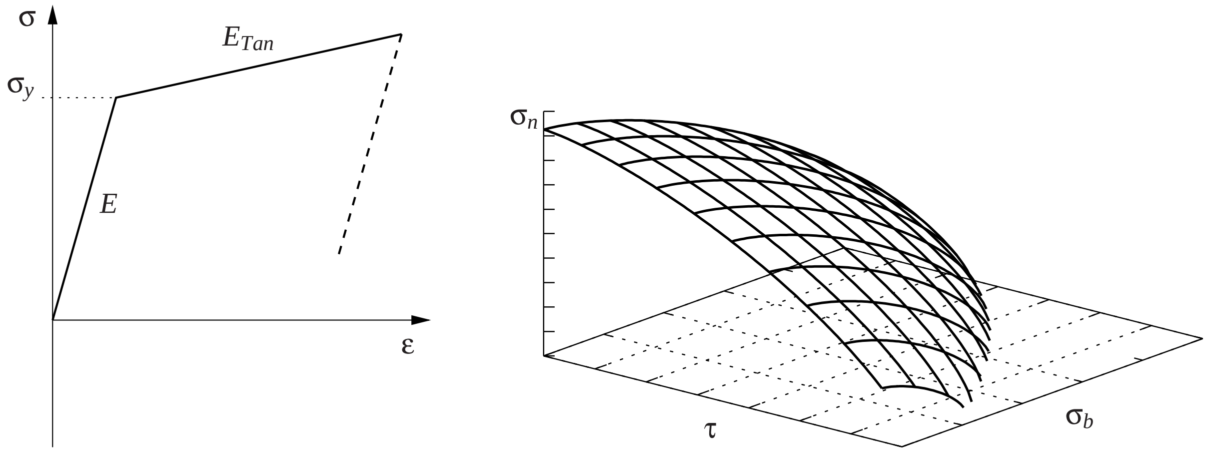

(a) Bi-linear elasto-plastic material model (b) Failure surface in $(\sigma_n, \sigma_b, \tau)$

Figure 5: Material and failure model of MAT_SPOTWELD_DA

The failure is taken into account by a stress based failure criterion (see Fig. 5b)

$$f = \left(\frac{\sigma_n}{S_n}\right)^{n_n} + \left(\frac{\sigma_b}{S_b}\right)^{n_b} + \left(\frac{\tau}{S_s}\right)^{n_s} \leq 1, \quad (3)$$

where S_n, S_b and S_s describe the failure parameters for normal stress σ_n, bending stress σ_b and shear stress τ, respectively. The failure surface can take any arbitrary shape controlled by the three exponents n_n, n_b and n_s, however, it is assumed that $n = n_n = n_b = n_s$.

4 Systematical Approach Concerning the Thickness

In the previous section, a method for deriving a detailed model for spot weld was presented. Now the model will be applied for a systematical analysis of the critical force at failure regarding the sheet thicknesses. This study helps to understand the failure mechanism and to improve the simplified model of spot welds finally. Similarly to the basic inputs of the detailed model, the influence of the sheet thickness regarding the dimension of the spot weld and the heat affected zone has to be studied first. Therefore, a cut with the corresponding Vickers hardness test was provided for a small series of several gage combinations, see Tab. 1.

		1.00	1.25	1.50	1.75	2.00
1.00	$ø_{SW}$	4.84		4.84		
	$ø_{HAZ}$	6.80		6.84		
1.25	$ø_{SW}$					
	$ø_{HAZ}$					
1.50	$ø_{SW}$			5.60		4.83
	$ø_{HAZ}$			7.60		7.72
1.75	$ø_{SW}$					
	$ø_{HAZ}$					
2.00	$ø_{SW}$					5.96
	$ø_{HAZ}$					9.47

Table 1: Test matrix with available hardness distribution of the spot weld

Theoretically, the spot weld should be manufactured with a diameter of $4\sqrt{\min(t_1,t_2)}$ to ensure a conservative prediction of the failure parameter in later simulations. Referring to the comparison of the measured and theoretical values of the spot weld diameter, some differences can be observed. Therefore following steps needs to be considered, which describe the methodology of deriving the systematical approach:

1. validation of the detailed spot weld model by means of the determined spot weld diameter and performed experiments on coupon level,
2. modeling and simulation of the whole test matrix in Tab. 1 for all gage combinations with the minimum diameter and the given approximations for the heat affected zone,
3. evaluation of the critical forces at spot weld failure,
4. determination the parameter for the simplified spot weld model,
5. derivation a systematical approach regarding the sheet thickness.

In the first step, the capability of the detailed modell regarding the gage combination 1.5 mm-1.5 mm will be proved using the real dimensions of the three sub-zones. Hence the simulation show a good correlation to the experiment, see Fig. 6, it is assumed that the detailed model represent the properties and the behavior of the spot weld precisely in the following steps.

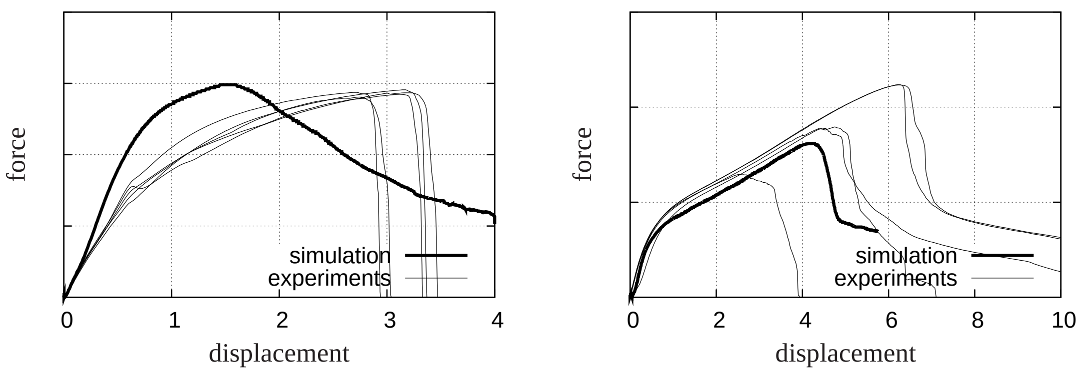

(a) KS2-0° (b) KS2-60°

Figure 6: Comparison of the detailed model with experiments for HL320LA on coupon level

On the basis of the determined dimension of the sub-zones, see Tab. 1, the diameter of the heat affected zone d_{HAZ} can be approximated by scaling the spot weld diameter d_{SW} via

$$d_{HAZ} = \alpha d_{SW} \qquad \text{with} \qquad \alpha \approx 1.5. \tag{4}$$

In combination with the material data, all required input data are provided to build the series of the detailed model. Now, the force-displacement characteristics of all gage combinations can be computed for all KS2-specimen and the coach peel. Later, the failure parameter for each combination can be calculated from the critical forces. Finally, the failure parameter are used for a systematical approach and an approximation. Hence only the sheet thickness was changed, the approximation is defined as a function of the minimal sheet thickness and of the difference of the sheet thickness in quadratic terms of

$$\begin{aligned}(S_N, S_B, S_S) &= f(t_1, t_2)\\ &= A\Delta t^2 + Bt\Delta t + Ct^2 + Dt + E\Delta t + F,\end{aligned}$$

with $\Delta t = \min(t_1, t_2)$ and $\Delta t = |t_1 - t_2|$. The parameter A, B, C, D, and E are determined by a least square optimization using the failure parameter of step 4.

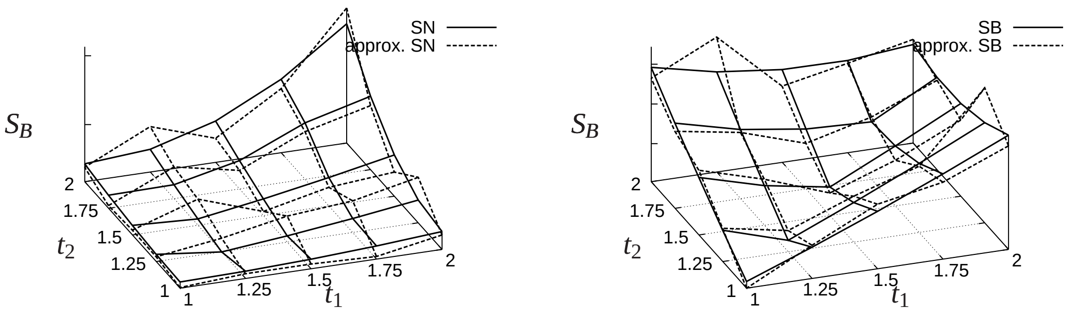

(a) (b)

Figure 7: Approximation of the failure parameter

Fig. 7 shows the approximation for the failure parameters S_N and S_B. In general, the correlation for the symmetrical combinations is acceptable, whereas the values for some unsymmetrical combinations should be improved. In the next steps, alternative formulations will be investigated to minimize the variations of the approximated failure parameters.

5 Dynamic Behavior

5.1 Validation for HT600XD

The effort of the experiments as well as the quality of the results increase strongly with the load speed subjected to the specimen. At higher load speed, approximately 2 m/s, oscillations of the clamping devices and the testing machine disturb the obtained force-displacement characteristic, see Fig. 9c. To prove the practicability, the feasibility of the modeling technique including the strain rate dependent Gurson material is studied with HT600XD.

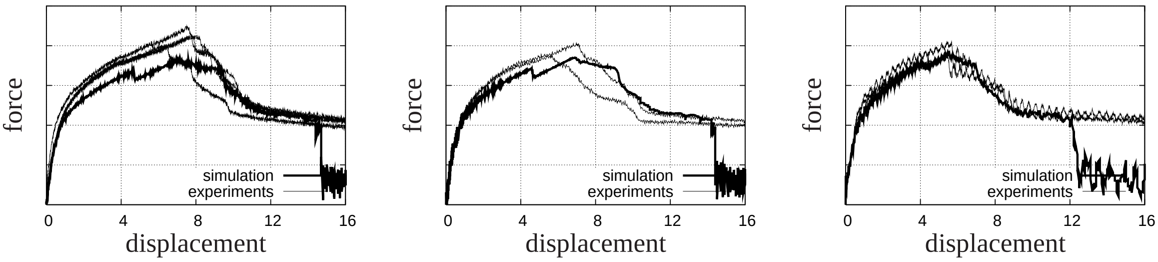

(a) $v = 0.02$ m/s (b) $v = 0.2$ m/s (c) $v = 2.0$ m/s

Figure 8: Coach peel: comparison of experiments and simulation for different load speeds

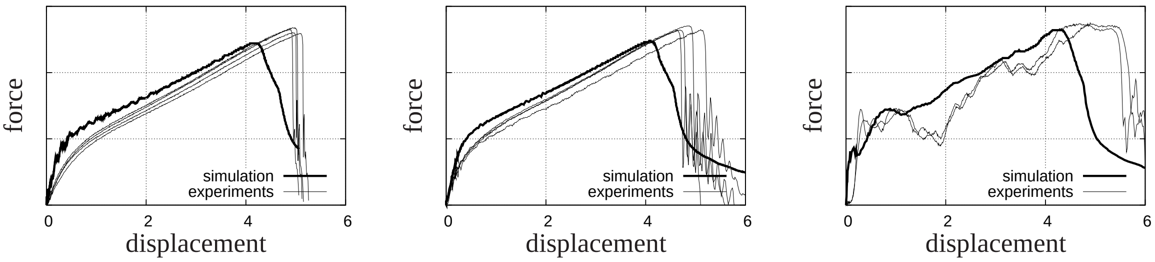

(a) $v = 0.02$ m/s (b) $v = 0.2$ m/s (c) $v = 2.0$ m/s

Figure 9: KS2-60°: comparison of experiments and simulation for different load speeds

The specimen made of HT600XD were subjected to load speed $v = qs, 0.02, 0.2, 2$ m/s. It can be seen that the correlation between the experiments and the simulation is good, see Fig. 8 and Fig. 9.

5.2 Prognosis for DC04

After the good correlation of experimental data and simulation results could be verified, the behavior of another spot welded material has to be investigated only with the detailed model. To ensure the correct approximation of the real dimension and condition a first comparison for the quasi-static load case is be performed. In the first step, the geometry was taken from a cut and the corresponding Vickers hardness test as described above. Afterwards, the spot weld is modeled with the smallest dimension of $d_{SW} = 4\sqrt{t_{\min}}$. This ensures a conservative estimation of the critical forces and displacements.

Fig. 10 shows the influence of the load speed and according the strain rate for different load angles. The abscissa and the ordinate represent the pure shear at 0° and pure tension at 90°, respectively. The critical forces at $v = 2$ m/s are up to 50% higher in comparison to the quasi-static values, whereas the influence of the load speed differs for all load angles. Finally, the results of this study can be taken now to implement the strain rate dependency into the simplified model.

6 Conclusion

In this paper, a methodology was presented to model the failure behavior of spot welds using a highly detailed model. The good correlation with experiments could be demonstrated for HL320LA as well as for HT600XD. On the basis of the proved model, a systematical analysis was performed to study

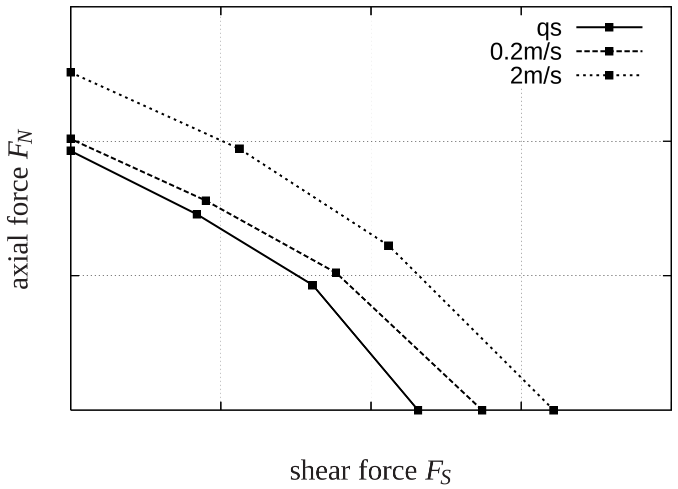

Figure 10: Critical force of DC04 dependent on the strain rate derived from the detailed spot weld model

the influence of the sheet thickness to the critical force at failure. Such investigations are the basis for improving the simplified model for spot weld later.

The method was further used to study the spot weld failure behavior at higher strain rates and load speeds. It can help to obtain the characteristic force-displacement curves for higher load speeds without any disturbing oscillations. At last, the strain rate dependence of the critical force was derived for DC04 and will be used to improve the simplified model.

Nevertheless, the presented methodology has still some deficits. Because of the utilization of Gurson's material model, the failure of the hexahedron elements due to shearing load can not be obtained. This can let to an incorrect modeling of the failure mechanism and to an overestimation of the critical force. In experiments, the failure mechanism switches from a pull-out to a tear-off rupture for higher sheet thicknesses and higher material strength, which can not be modeled in the simulation. With a new or modified material model covering failure due to tensile and shearing load, the overall correlation of the detailed model could be improved.

References

[1] Blanquet, M. *Detailed Modelling of Spot Welded Joints Concerning Dynamic Behaviour*, Diplom-Thesis, Daimler AG / University Valienciennes 2008

[2] M. Feucht, W. Faßnacht, *Simulation der duktilen Rissbildung in Crashberechnungen mit Hilfe des Gurson-Modells*, 17. CADFEM Users meeting, III-4.3, Sonthofen 1999

[3] Feucht, M.,*Recent development and applications of the Gurson model*, LS-DYNA Anwenderforum, Ulm 2006

[4] Gurson, A. L., *Continuum theory of ductile rupture by void nucleation and growth. Part I Yield criteria and flow rules for porous ductile media.*, Journal of engineering Material and Technology, 1977, 99, 2-15.

[5] Lamouroux, E. H. J. Modélisation détaillé des soudures par point et Laser pour simuler la rupture des assemblages automobiles. PhD-Thesis, Laboratoire LAMIH, Valenciennes 2007

[6] Michel, G., *Simplified Modelling of Spot Welded Joints Simulating the Failure of Car Assemblies*, DRT-Thesis, Daimler AG / University Valienciennes 2008

[7] Needleman, A., Tvergaard, V.,*Analysis of Ductile Rupture in Notched Bars*, J. Mech. Phys. Solids 32, pp. 461-490, 1984.

[8] Seeger, F., Feucht, M., Frank. Th., Keding, B., Haufe, A., *An Investigation on Spot Weld Modelling for Crash Simulation with LS-Dyna*, 4. LS-Dyna User Conference, Bamberg 2005

[9] Sommer S., Sun D.-Z., *Ersatzmodelle für Punktschweißverbindungen in der Crashsimulation*, VDI-Berichte Nr. 1967.2, p 543 - 554

[10] Sommer S., Andrieux F., Memhard D., Sun D.-Z., *Modellierung des Verformungs- und Versagensverhaltens von Punktschweiß - und Klebverbindungen unter Crashbelastung*, Tagungsband DVM-Tag 2008